Available online at www.sciencedirect.com

ScienceDirect

Mendeleev Commun., 2024, **34**, 321–324

Mendeleev Communications

Theoretical assessment of chloride ion influence on grain growth of hybrid perovskites

Ekaterina I. Marchenko,[a,b] Nikolay A. Belich,[a] Anastasia V. Iosimovska,[b] Vladimir A. Misyutin,[a] Eugene A. Goodilin[a,c] and Alexey B. Tarasov*[a,c]

[a] *Department of Materials Science, M. V. Lomonosov Moscow State University, 119991 Moscow, Russian Federation. E-mail: alexey.bor.tarasov@yandex.ru*
[b] *Department of Geology, M. V. Lomonosov Moscow State University, 119991 Moscow, Russian Federation*
[c] *Department of Chemistry, M. V. Lomonosov Moscow State University, 119991 Moscow, Russian Federation*

DOI: 10.1016/j.mencom.2024.04.004

Theoretical assessment of Cl-excessive, mixed-halide grain boundaries in hybrid perovskite thin films demonstrates that ordered 3D/2D interfaces along perovskite (100) crystallographic planes are the most energetically favored among other possible cases.

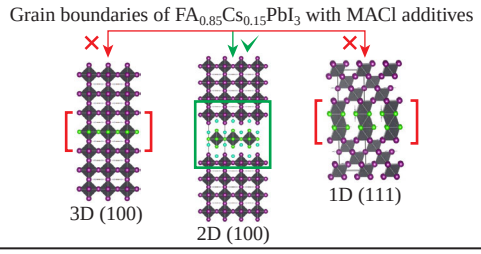

Keywords: thermodynamic stability, phase transition energy, hybrid perovskites, polytypes, chloride ion additives, grain boundaries, interfaces.

Hybrid halide perovskites ABX_3[†] have attracted significant interest due to their exceptional performance in various optoelectronic applications, mostly as light-absorbing layers in perovskite solar cells.[1–7] Perovskite solar cells have been announced in 2009 with power conversion efficiency (PCE) reaching 3.8%,[7] and device performance has been dramatically improved over the past decade, currently exceeding 26.1%,[8] thus proving the great potential of these solar cells for future practical applications.

Despite promising trends in improving PCE, the problem of poor long-term stability, among others, must be overcome before commercialization of these devices.[9,10] Compositional engineering of perovskite layers has recently emerged as an effective approach to improve device stability without compromising power efficiency.[11–16] In this context, mixing A-site cations of different sizes has been used to produce solar cells with improved operational stability.[12,14–17] In particular, $(FA_{1-x}Cs_x)PbI_3$ ($x < 0.15$) solid solution films are one of the most promising materials for light-absorbing layers, ensuring high operational stability of perovskite solar cells.[18]

Certain chloride compounds added to the perovskite precursor solution are known to improve the quality of hybrid perovskite thin films, often resulting in record-breaking efficiency.[19–23] However, the role of excess chlorides in the formation of hybrid perovskite films has not yet been sufficiently investigated. The study of this issue has two aspects: (i) identification of possible chloride-containing intermediate phases and their influence on the formation of thin films of hybrid perovskite; (ii) identification of crystal chemical and grain growth aspects of the influence of chloride ions on the morphology of thin films after thermal treatment. A few studies have been published elucidating chloride-containing perovskite intermediate phases and the process of their transformation into final perovskites.[19,24] At the same time, it has been experimentally established that the improvement in morphology and crystallinity largely depends on the amount of incorporated chloride compounds, which affects the PCE and operational stability of perovskite solar cells.[21,25,26] However, questions and conflicting conclusions remain regarding the identification of the crystal chemical role of chloride ions. It has been repeatedly shown that, regardless of the ratio of components in the precursor solution, the incorporation of chloride ions into the halide sublattice occurs only to relatively low levels (below 3–4 at%).[27] The strong difference in the ionic radii of the halogens prevents the formation of a continuous solid solution and keeps the material's band gap essentially unchanged, while the incorporation of chloride ions dramatically improves charge transport within the perovskite layers.[27] The reason is that after annealing of perovskite films, chloride ions are not identified in the bulk, but are concentrated at the grain boundaries.[28] These findings require the analysis of three possible cases: (i) a uniformly distributed disordered or ordered solid solution containing iodine sites with a mixed I^-/Cl^- occupancy, (ii) an ordered 3D/2D interface between perovskite grains along the (100) crystallographic planes of the perovskite, (iii) an ordered 3D/1D interface between perovskite grains, represented by alternating blocks of the perovskite structure with hexagonal δ-phases [(111) interfaces].

Here, we theoretically assessed these cases for the most popular hybrid halide perovskite $(FA_{1-x}Cs_x)PbI_3$ ($x \leqslant 0.15$) with an excess content of chloride ions by calculating the relative thermodynamic stability of such heterostructures and the most stable grain interfaces, which was further confirmed by experimental synthesis. To the best of our knowledge, this is the first report on the interfacial stability of different types of perovskite grains.

In this work, the development of a model of classical force field interatomic potentials and all the calculations under constant

[†] In this formula, A is a monovalent cation such as Cs^+, methylammonium $MeNH_3^+$ (MA) or formamidinium $[HC(NH_2)_2]^+$ (FA), B is a divalent cation such as Pb^{2+} or Sn^{2+}, and X is iodide, bromide or chloride ions.

pressure conditions were performed using the GULP program[29] and a previously published technique for fitting interatomic potentials.[30,31] The model of interatomic potentials was fitted according to the unit cell geometry, atomic coordinates and experimentally assessed elastic properties. To fit the parameters of the pair interatomic potential model, the following phases were used: α-$CsPbI_3$, δ-$CsPbI_3$, α-$CsPbCl_3$, $Cs_2PbI_2Cl_2$,[32] α-$FAPbI_3$ and δ-$FAPbI_3$. The .cif files of these structures were taken from the Materials Project database.[33] The starting values of the pair interatomic interaction potentials, which were used for the further optimization procedure, were taken from previously published articles.[30,34] The relative energies of the polymorphs at different temperatures were also compared to consider phase transitions consistent with experimental data.

According to the priority growth directions of hybrid perovskite crystals of $FA_{0.85}Cs_{0.15}PbI_3$ composition in thin films, using the VESTA program,[35] we constructed two types of Cl-excessive interfaces: (100) and (111) oriented interfaces along the perovskite crystallographic planes. It is worth noting that the formation of extended Cl-excessive defects in the (100) plane can lead to a reduction in the dimensionality of the crystal structure and the appearance of a 'layered' Ruddlesden–Popper (RP)[36] phase of $Cs_2PbI_2Cl_2$, which was experimentally detected earlier.[32] The (111) interfaces represent planes of cubic close packing in hybrid perovskites, modification of the densely packed layers of which leads to the formation of various hexagonal close-packed polytypes.[37] We designed four (100) interfaces [Figure 1(*a*)], the first three of which, (100)-1, (100)-2 and (100)-3, are interfaces where the structural block of the low-dimensional phase of the RP type structure is located between layers with different concentrations and ordering of chloride ions, and cesium ions are located between octahedral layers. Heterostructure (100)-4 is a cubic perovskite supercell with a single atomic layer of chloride ions along the (100) plane, thus simulating an ordered I–Cl solid solution in cubic perovskite. Analogously to interfaces (100), we also constructed interfaces (111) [Figure 1(*b*)]. Thus, heterostructures (111)-1, (111)-2, (111)-3 and (111)-4 are characterized by the incorporation of grain-boundary lead halide octahedra, simulating the experimentally observed incorporation of chloride ions into impurity delta phases on the defect boundary between perovskite crystals. The constructed supercells contain 1140 atoms and differ in the content of chlorine and cesium in the defective interface region, as shown in Figure 1.

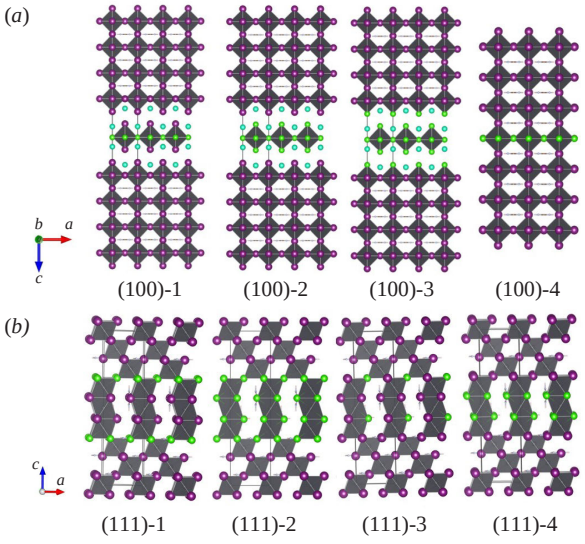

Figure 1 Theoretically constructed possible interfaces in hybrid perovskite crystals containing an excess of chloride ions: (*a*) (100) and (*b*) (111) heterostuctures.

In order to examine the relative thermodynamic stability of different possible ordered heterostructures of the $(FA_{0.85}Cs_{0.15})PbI_3$ perovskite with $Cl^- \rightarrow I^-$ impurities between perovskite grains, the total energy of the constructed interfaces was calculated (Figure 2). All hypothetical interfaces are less stable relative to the α-$FAPbI_3$ perovskite phase. However, two different trends are observed depending on the type of stacking of the (100) or (111) structural blocks [Figure 2(*a*)]. The results of relative energy calculations showed that the (100)-ordered 3D/2D interface of the perovskite $FAPbI_3$–'RP' stacking of structural blocks with Cs^+ and Cl^- excess region of heterostructures (100)-1, (100)-2 and (100)-3 [see Figure 2(*a*)] is energetically more preferable than all other constructed (100)-4 and (111) interfaces. Surprisingly, the energy of interfaces (100)-1, (100)-2 and (100)-3 does not become much different with increasing content of chloride ions, remaining in the range of 0.01–0.07 eV per atom [Figure 2(*b*)], and at the same time it certainly differs from the energy of the α-$FAPbI_3$ perovskite by 0.04–0.11 eV per atom. It is interesting to note that heterostructure (100)-1 with ordered chloride ions resembles the $Cs_2PbI_2Cl_2$ phase[32] with similar energy data compared to α-$FAPbI_3$. In contrast to the (100) heterostructures, all constructed hypothetical 3D/1D (111) interfaces with additional chloride and cesium ions are significantly less favorable in energy relative to the α-$FAPbI_3$ perovskite (more than 1 eV per atom). The ordering of chloride ions in the 3D bulk structure of the α-$FAPbI_3$ perovskite in the case of interface (100)-4 is also energetically unfavorable [see Figure 2(*a*)]. Thus, based on the results of our calculations, we have shown that chloride ions effectively passivate the close-packed, flattest (100) boundaries of perovskite grains during the formation of a 3D/2D heterostructure. This result is also supported by crystal chemical considerations, since the ratio of the ionic radii of chlorine and lead prevents connecting $PbCl_6$ octahedra along the faces in hybrid lead chlorides, and they are indeed connected only at the vertices, which is consistent with the results of this work.

To compare the results of theoretical modeling with experimental data, thin films of hybrid perovskite with the composition $FA_{0.85}Cs_{0.15}PbI_3$ were synthesized using varying amounts (0, 13.3 and 26.7%) of methylammonium chloride (MACl) additive. Thin films were annealed at different temperatures (125, 150 and

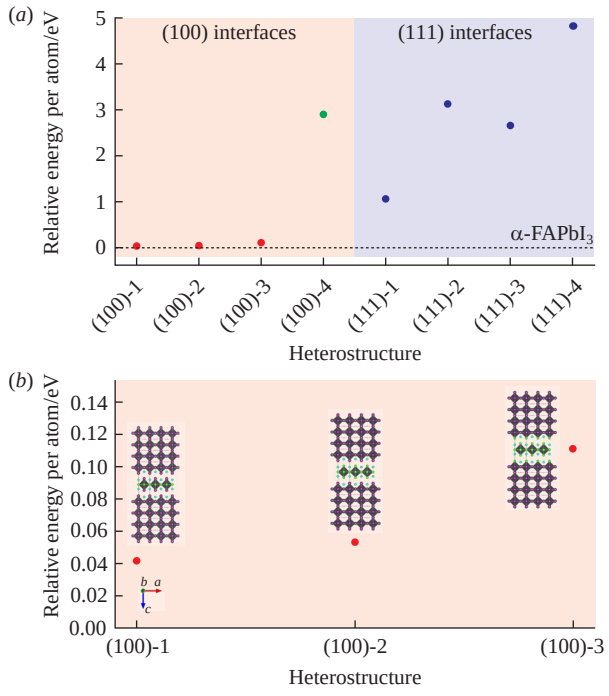

Figure 2 Calculated relative energies of possible hybrid perovskite ordered heterostructures with excess Cl defects: (*a*) all calculated interfaces and (*b*) different (100)-only configurations.

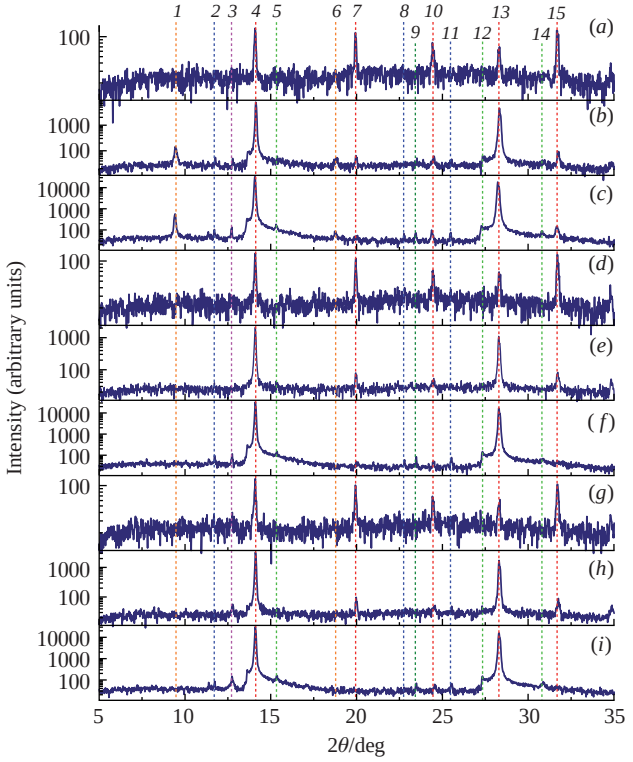

Figure 3 XRD patterns of $FA_{0.85}Cs_{0.15}PbI_3$ samples annealed at (*a*)–(*c*) 125, (*d*)–(*f*) 150 and (*g*)–(*i*) 175 °C (*a*),(*d*),(*g*) without and with (*b*),(*e*),(*h*) 13.33 and (*c*),(*f*),(*i*) 26.67% MACl additive. The dashed lines indicate the positions of the reflection peaks for (*1*) $Cs_2PbI_2Cl_2$ (002), (*2*) δ-$FAPbI_3$ (100), (*3*) PbI_2 (001), (*4*) α-$FAPbI_3$ (100), (*5*) $FAPbCl_3$ (010), (*6*) $Cs_2PbI_2Cl_2$ (004), (*7*) α-$FAPbI_3$ (110), (*8*) δ-$FAPbI_3$ (002), (*9*) FACl (121), (*10*) α-$FAPbI_3$ (111), (*11*) δ-$FAPbI_3$ (102), (*12*) $FAPbCl_3$ (111), (*13*) α-$FAPbI_3$ (200), (*14*) $FAPbCl_3$ (200) and (*15*) α-$FAPbI_3$ (210).

175 °C) for 25 min.‡ Analysis of X-ray diffraction (XRD) data (Figure 3) showed the presence of lead iodide impurity in all films annealed at 175 °C, associated with partial decomposition of perovskite due to the evaporation of organic components. Additionally, the admixture of PbI_2 was detected in films with the highest (26.7%) amount of the MACl additive at each annealing temperature.

When synthesized at 125 °C, thin films with the MACl additives contain impurities of FACl (2θ = 23.35–23.50°) and $FAPbCl_3$ (2θ = 15.15–15.50°), as well as the RP phase $Cs_2PbI_2Cl_2$ (2θ = 9.35–9.50°). Moreover, the intensity of its (002) reflection increases with increasing amount of the MACl additive.

Upon annealing at 150 and 175 °C, the impurity phase $Cs_2PbI_2Cl_2$ was not detected, possibly due to its decomposition at these temperatures. In thin films with the highest (26.67%) MACl additive content, impurities of the perovskite δ-phase are also observed. It is worth noting that the intensity of the (100) reflections of perovskite increases significantly with increasing amount of the MACl additive, and the content of the $Cs_2PbI_2Cl_2$ impurity phase also increases. Furthermore, the position of the maximum of the perovskite peak in the photoluminescence spectra does not depend on the amount of the MACl additive and the annealing temperature, which indicates that the incorporation of chloride ions into the iodine sites of perovskites does not occur.

Thus, based on theoretical calculations and taking into account experimental data, it should be concluded that excess chloride and cesium ions passivate the (100) faces of perovskite crystallites, forming 3D/2D ordered interfaces. Further research will be aimed at investigating the formation energies of point defects as a result of the incorporation of Cl^- at the interfaces of perovskite grains and their impact on the optoelectronic characteristics of the material.

This work was carried out within the framework of the state assignment of the Ministry of Science and Higher Education of the Russian Federation (theme no. 122040100043-1). XRD studies were performed using the equipment of the Joint Research Centre for Physical Methods of Research of the Kurnakov Institute of General and Inorganic Chemistry of the Russian Academy of Sciences (JRC PMR IGIC RAS).

‡ Perovskite precursor solutions were prepared from formamidinium iodide (CH_5N_2I, 98%, Dyesol), cesium iodide (CsI, >99.999%, Tokyo Chemical Industry), lead iodide (PbI_2, 99.999%, Lanhit), using dimethylformamide (DMF, anhydrous, >99.8%, Sigma-Aldrich), dimethyl sulfoxide (DMSO, anhydrous, >99.8%, Sigma-Aldrich) and chlorobenzene (CB, >99.8%, Sigma-Aldrich). A 1.5 M $FA_{0.85}Cs_{0.15}PbI_3$ precursor solution with an excess amount (13.33 and 26.67%) of MACl was prepared in a nitrogen-filled glovebox using a mixture of DMF–DMSO (4 : 1, v/v) and then stirred at 60 °C for 60 min and at room temperature for 30–90 min before deposition. The perovskite precursor solution was spin-coated at 6000 rpm for 30 s, with CB antisolvent dripping 25 s before the end of the program. The temperature in the glovebox was set between 24 and 26 °C. XRD measurements were carried out on a Bruker D8 Advance diffractometer (Cu Kα, λ = 0.154060 Å) in the range 2θ = 5–35° with a step of 0.02° and a step time of 0.1 s.

References

1 H. Wang and D. H. Kim, *Chem. Soc. Rev.*, 2017, **46**, 5204.
2 S. Adjokatse, H.-H. Fang and M. A. Loi, *Mater. Today*, 2017, **20**, 413.
3 G. Xing, N. Mathews, S. S. Lim, N. Yantara, X. Liu, D. Sabba, M. Grätzel, S. Mhaisalkar and T. C. Sum, *Nat. Mater.*, 2014, **13**, 476.
4 S. D. Stranks and H. J. Snaith, *Nat. Nanotechnol.*, 2015, **10**, 391.
5 J.-P. Correa-Baena, M. Saliba, T. Buonassisi, M. Grätzel, A. Abate, W. Tress and A. Hagfeldt, *Science*, 2017, **358**, 739.
6 M. Grätzel, *Nat. Mater.*, 2014, **13**, 838.
7 A. Kojima, K. Teshima, Y. Shirai and T. Miyasaka, *J. Am. Chem. Soc.*, 2009, **131**, 6050.
8 Z. Liang, Y. Zhang, H. Xu, W. Chen, B. Liu, J. Zhang, H. Zhang, Z. Wang, D.-H. Kang, J. Zeng, X. Gao, Q. Wang, H. Hu, H. Zhou, X. Cai, X. Tian, P. Reiss, B. Xu, T. Kirchartz, Z. Xiao, S. Dai, N.-G. Park, J. Ye and X. Pan, *Nature*, 2023, **624**, 557.
9 D. Bryant, N. Aristidou, S. Pont, I. Sanchez-Molina, T. Chotchunangatchaval, S. Wheeler, J. R. Durrant and S. A. Haque, *Energy Environ. Sci.*, 2016, **9**, 1655.
10 T. A. Berhe, W.-N. Su, C.-H. Chen, C.-J. Pan, J.-H. Cheng, H.-M. Chen, M.-C. Tsai, L.-Y. Chen, A. A. Dubale and B.-J. Hwang, *Energy Environ. Sci.*, 2016, **9**, 323.
11 N. J. Jeon, J. H. Noh, W. S. Yang, Y. C. Kim, S. Ryu, J. Seo and S. I. Seok, *Nature*, 2015, **517**, 476.
12 N. Pellet, P. Gao, G. Gregori, T.-Y. Yang, M. K. Nazeeruddin, J. Maier and M. Grätzel, *Angew. Chem., Int. Ed.*, 2014, **53**, 3151.
13 M. Saliba, T. Matsui, J.-Y. Seo, K. Domanski, J.-P. Correa-Baena, M. K. Nazeeruddin, S. M. Zakeeruddin, W. Tress, A. Abate, A. Hagfeldt and M. Grätzel, *Energy Environ. Sci.*, 2016, **9**, 1989.
14 D. P. McMeekin, G. Sadoughi, W. Rehman, G. E. Eperon, M. Saliba, M. T. Hörantner, A. Haghighirad, N. Sakai, L. Korte, B. Rech, M. B. Johnston, L. M. Herz and H. J. Snaith, *Science*, 2016, **351**, 151.
15 R. G. Niemann, L. Gouda, J. Hu, S. Tirosh, R. Gottesman, P. J. Cameron and A. Zaban, *J. Mater. Chem. A*, 2016, **4**, 17819.
16 W. Rehman, D. P. McMeekin, J. B. Patel, R. L. Milot, M. B. Johnston, H. J. Snaith and L. M. Herz, *Energy Environ. Sci.*, 2017, **10**, 361.
17 C. Yi, J. Luo, S. Meloni, A. Boziki, N. Ashari-Astani, C. Grätzel, S. M. Zakeeruddin, U. Röthlisberger and M. Grätzel, *Energy Environ. Sci.*, 2016, **9**, 656.
18 P. Luo, S. Zhou, Y. Zhou, W. Xia, L. Sun, J. Cheng, C. Xu and Y. Lu, *ACS Appl. Mater. Interfaces*, 2017, **9**, 42708.
19 S. Takahashi, S. Uchida and H. Segawa, *ACS Omega*, 2023, **8**, 42711.
20 H. Min, M. Kim, S.-U. Lee, H. Kim, G. Kim, K. Choi, J. H. Lee and S. I. Seok, *Science*, 2019, **366**, 749.
21 M. Kim, G.-H. Kim, T. K. Lee, I. W. Choi, H. W. Choi, Y. Jo, Y. J. Yoon, J. W. Kim, J. Lee, D. Huh, H. Lee, S. K. Kwak, J. Y. Kim and D. S. Kim, *Joule*, 2019, **3**, 2179.
22 M. M. Tavakoli, P. Yadav, D. Prochowicz, M. Sponseller, A. Osherov, V. Bulović and J. Kong, *Adv. Energy Mater.*, 2019, **9**, 1803587.

23 Q. Li, Y. Zhao, R. Fu, W. Zhou, Y. Zhao, X. Liu, D. Yu and Q. Zhao, *Adv. Mater.*, 2018, **30**, 1803095.
24 K. H. Stone, A. Gold-Parker, V. L. Pool, E. L. Unger, A. R. Bowring, M. D. McGehee, M. F. Toney and C. J. Tassone, *Nat. Commun.*, 2018, **9**, 3458.
25 B. Lee, T. Hwang, S. Lee, B. Shin and B. Park, *Sci. Rep.*, 2019, **9**, 4803.
26 N. D. Pham, V. T. Tiong, P. Chen, L. Wang, G. J. Wilson, J. Bell and H. Wang, *J. Mater. Chem. A*, 2017, **5**, 5195.
27 S. Colella, E. Mosconi, P. Fedeli, A. Listorti, F. Gazza, F. Orlandi, P. Ferro, T. Besagni, A. Rizzo, G. Calestani, G. Gigli, F. De Angelis and R. Mosca, *Chem. Mater.*, 2013, **25**, 4613.
28 J. Jeong, M. Kim, J. Seo, H. Lu, P. Ahlawat, A. Mishra, Y. Yang, M. A. Hope, F. T. Eickemeyer, M. Kim, Y. J. Yoon, I. W. Choi, B. P. Darwich, S. J. Choi, Y. Jo, J. H. Lee, B. Walker, S. M. Zakeeruddin, L. Emsley, U. Rothlisberger, A. Hagfeldt, D. S. Kim, M. Grätzel and J. Y. Kim, *Nature*, 2021, **592**, 381.
29 J. D. Gale and A. L. Rohl, *Mol. Simul.*, 2003, **29**, 291.
30 E. I. Marchenko, S. A. Fateev, A. A. Petrov, E. A. Goodilin, N. N. Eremin and A. B. Tarasov, *J. Phys. Chem. C*, 2019, **123**, 26036.
31 E. I. Marchenko, S. A. Fateev, A. A. Petrov, E. A. Goodilin and A. B. Tarasov, *Mendeleev Commun.*, 2020, **30**, 279.
32 J. Li, Q. Yu, Y. He, C. C. Stoumpos, G. Niu, G. G. Trimarchi, H. Guo, G. Dong, D. Wang, L. Wang and M. G. Kanatzidis, *J. Am. Chem. Soc.*, 2018, **140**, 11085.
33 A. Jain, S. P. Ong, G. Hautier, W. Chen, W. D. Richards, S. Dacek, S. Cholia, D. Gunter, D. Skinner, G. Ceder and K. A. Persson, *APL Mater.*, 2013, **1**, 011002.
34 J. A. Seijas-Bellido, B. Samanta, K. Valadez-Villalobos, J. J. Gallardo, J. Navas, S. R. G. Balestra, R. M. Madero Castro, J. M. Vicent-Luna, S. Tao, M. Caspary Toroker and J. A. Anta, *J. Chem. Inf. Model.*, 2022, **62**, 6423.
35 K. Momma and F. Izumi, *J. Appl. Crystallogr.*, 2011, **44**, 1272.
36 S. N. Ruddlesden and P. Popper, *Acta Crystallogr.*, 1957, **10**, 538.
37 E. I. Marchenko, S. A. Fateev, V. V. Korolev, V. Buchinskiy, N. N. Eremin, E. A. Goodilin and A. B. Tarasov, *J. Mater. Chem. C*, 2022, **10**, 16838.

Received: 26th December 2023; Com. 23/7351